Journal of Asian Earth Sciences 227 (2022) 105080

Contents lists available at ScienceDirect

Journal of Asian Earth Sciences

journal homepage: www.elsevier.com/locate/jseaes

Reconstruction of the late Holocene climate variability from the summer monsoon dominated Bhagirathi valley, western Himalaya

Ipsita Roy [a], Parminder Singh Ranhotra [a,*], Nidhi Tomar [a], Mayank Shekhar [a], Shailesh Agrawal [a], Amalava Bhattacharyya [a], Pankaj Kumar [b], Shiva Kumar Patil [c], Rajveer Sharma [b]

[a] Birbal Sahni Institute of Palaeosciences, 53, University Road, Lucknow 226007, India
[b] Inter-University Accelerator Centre, Near Vasant Kunj, New Delhi 110067, India
[c] KSKGRL, Indian Institute of Geomagnetism, Jhunshi, Prayagraj 211019, India

ARTICLE INFO

Keywords:
4.2 ka event
Medieval Warm Period
Little ice age
Palynology
Carbon Isotope
Magnetic Susceptibility

ABSTRACT

This study presents a centennial to decadal scale late Holocene climate scenario from the Indian summer monsoon (ISM) dominated region of western Himalaya. The subsurface sediments analyzed for palynology, carbon isotope ($\delta^{13}C_{org}$) and magnetic susceptibility (χlf) were collected from the temperate and alpine meadows, respectively receiving high (low) and relatively low (high) amount of ISM (winter) precipitation. We could identify the dry and moist phases linked to respective weakening and strengthening of ISM. High frequency of steppe pollen (*Ephedra*, Amaranthaceae, Asteraceae, Brassicaceae) between 4.4 and 3.8 ka represented a dry phase, coeval to 4.2 ka global dry event. Subsequent low $\delta^{13}C$ values and high pollen frequency of moist vegetation (Geraniaceae, Cyperaceae, Apiaceae, Ranunculaceae and pteridophytes) till ca. 0.9 ka suggested moist phase but with an intermittent dry episode ca. 2.9–2.5 ka, allowing rise of steppe taxa. Climate ameliorated ca. 1.8 ka and moist conditions further enhanced between 1.5 and 0.9 ka, corresponding to Medieval Warm Period. Sharp increase in $\delta^{13}C_{org}$ values and steppe vegetation ca. 0.8 ka attributed to dryness that intensified between 0.6 and 0.2 ka and coincide with Little Ice Age (LIA) anomaly. The recorded dry (weak ISM) phases showed correspondence with the low solar irradiance and supported the teleconnection with north Atlantic circulations. Palynological data from both the valleys complement each other throughout late Holocene time. However, the valleys showed temporal inconsistency in their aridity peaks during LIA phase. This indicates response variability of the two physiographically different sites to summer and winter monsoon systems.

1. Introduction

Extreme climatic conditions such as droughts and floods leave a profound impact on the socio-economics of any region. The Holocene epoch has been studied widely for its climate variability and the underlying driving mechanisms (Bradley et al., 2003; Lamb, 1965; Mann et al., 2009; Mayewski et al., 2004) that concern future climatic instability (Park et al., 2019) in response to post industrial global temperature rise. Late Holocene time period has been experiencing a declining trend of the extraterrestrial insolation (Berger and Loutre, 1999) and also the dry climatic episodes (Nesje and Dahl, 2003; Rowan, 2017). This time period has been vigorously investigated for the abrupt and short lived climatic events such as 4.2 ka, Medieval Warm Period (MWP) and Little Ice Age (LIA), and their asynchronicity on regional scale (Crowley and Lowery, 2000; Grove, 2001; Lamb, 1965; Mann et al., 2009; Park et al., 2019; Ran and Chen, 2019). The 4.2 ka event was marked by intense aridity of global extent (Booth et al., 2005; Fisher et al., 2008; Kaniewski et al., 2018; Wanner et al., 2015). Many important cultures and civilizations in Asia (Chang, 1999; Dixit et al., 2014; Liu and Feng, 2012), Mesopotamia (Cullen et al., 2000) and Egypt (Marshall et al., 2011) declined abruptly either directly or indirectly with the 4.2 ka event (Ran and Chen, 2019). Moreover, abrupt cooling has also been evidenced at 3.2 ka and 2.8 ka in the Mediterranean and Eurasian parts that substantially influenced the environment and ancient societies (Park et al., 2019 and references there in).

The Himalayan region from east to northwest is a complex of Indian summer monsoon (ISM), and the winter monsoon by westerly disturbances (WD) (Dimri et al., 2013; Dimri and Mohanty, 2009; Polanski

* Corresponding author.
E-mail address: parmindersingh_ranhotra@bsip.res.in (P.S. Ranhotra).

https://doi.org/10.1016/j.jseaes.2022.105080
Received 2 April 2021; Received in revised form 21 December 2021; Accepted 1 January 2022
Available online 5 January 2022
1367-9120/© 2022 Elsevier Ltd. All rights reserved.

et al., 2014). The region provides unique archives for inferring the past climate anomalies (Bhattacharyya et al., 2011; Demske et al., 2009; Kar et al., 2002; Kotlia et al., 2015; Liang et al., 2015; Phadtare, 2000; Ranhotra et al., 2018; Rawat et al., 2015; Sanwal et al., 2013; Srivastava et al., 2017; Vishnu-Mittre and Sharma, 1984). The total precipitation including the summer and winter precipitation, over the Himalaya, shows an inverse relation with that over the core ISM areas of Indian subcontinent (Kripalani et al., 2003). Also, the available proxy based past climate reconstruction records from the ISM dominant regions of the Indian subcontinent are not in correspondence with palaeo-records of the WD influenced Himalayan regions (Dimri et al. 2016; Kotlia et al., 2012, 2015; Sanwal et al., 2013). The ISM precipitation during mid to late Holocene showed decreasing strength connected to a southward shift of Inter Tropical Convergence Zone (ITCZ) (Gupta et al., 2003). This weakening trend of ISM corresponds to a decrease in the northern hemisphere insolation induced by precision-paced orbital forcing (Dimri et al., 2016). We assume that the interplay of WDs and ISM systems might have influenced the intensity and occurrence of the abrupt short lived late Holocene records over the Himalayan region. Also the complex regional topography and local orographic rains in the region modulate the hydrology of the region. Available climate reconstructions have provided information on climatic changes during Holocene (Draganits et al., 2014; Srivastava et al., 2017) or beyond (Ali et al., 2018; Demske et al., 2009; Ranhotra et al., 2018; Rawat et al., 2015). A few short lived climatic anomalies of late Holocene such as 2.8 ka event (Martin-Puertas et al., 2012) are subdued in most of the records. Also, the climate variability corresponding to globally arid 4.2 ka event was recorded by studies from different Himalayan regions (Ghosh et al., 2015; Leipe et al., 2014; Rawat et al., 2015). The event however remained variable and weakly resolved in the several sedimentary archives. Moreover, the late Holocene climate anomalies were less focused on their spatial synchronicity within the Himalayan region. This was either due to poor temporal resolution of the samples or indistinct response of the archives to climate change. Here we present the late Holocene vegetation and climatic changes resolved on a centennial to decadal scale from the moist temperate zone and the comparatively less moist alpine zone. Both the study sites are located in the ISM dominated region of western Himalaya and also receive the precipitation through WDs in winter months. The reconstructed late Holocene climatic events from both the sites have been compared for their synchronicity and temporal extent to better understand the influence of ISM-WD interplay across the region.

2. Study area

The study sites are Nachiketa (NAT; 30°38′N and 78°28′E) near Uttarkashi, and Bhojbasa Kame Terrace (KMT) in the Gangotri valley (KMT; 30°45′–31°15′ N and 78°54′–79°17′ E). Both the study sites are located at different altitudes in the valleys with variable precipitation (Fig. 1). The measured records of climate are not available due to lack of weather stations at both the sites. However, temperature and precipitation records for both the sites NAT (30.75°N; 78.25°E grid point) and KMT (climatic grid boundary ranging from 30.45–31.15°N; 78.54–79.17°E) were obtained from the Climatic Research Unit,

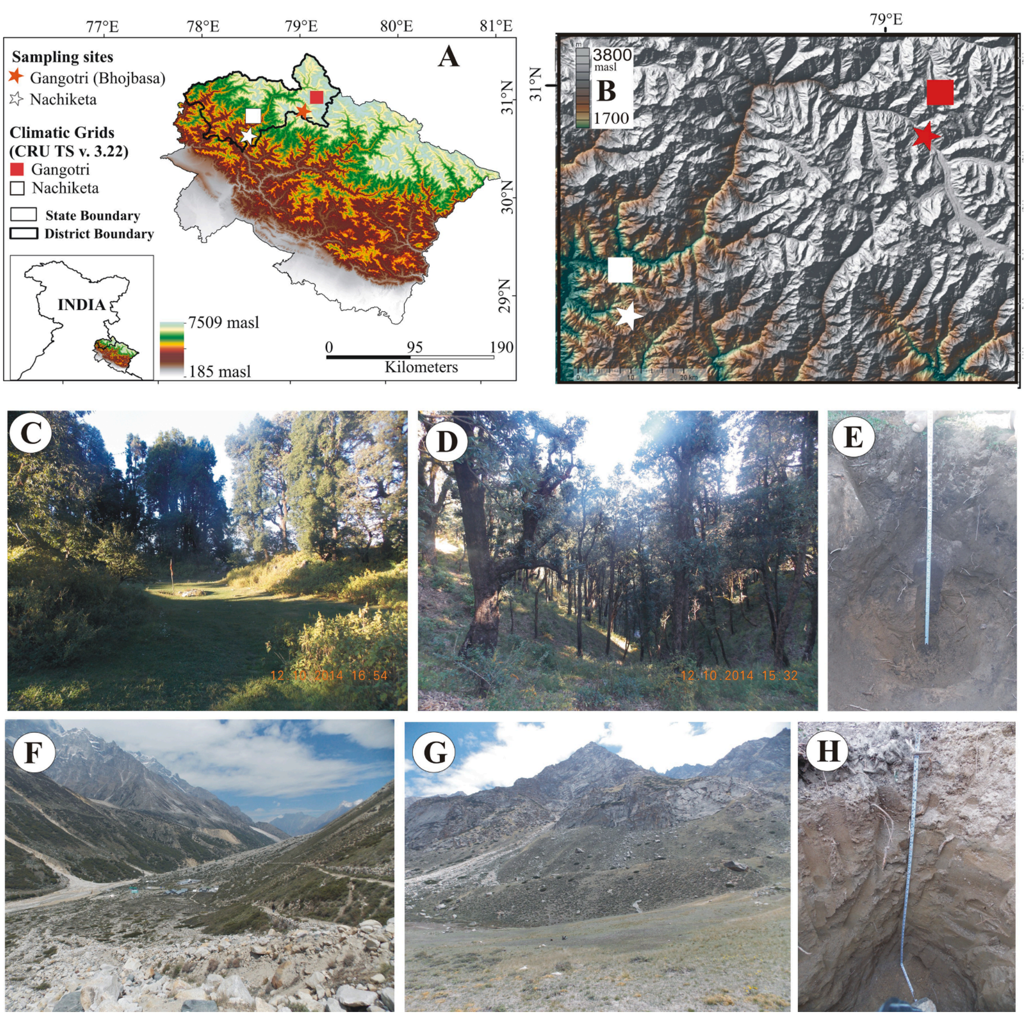

Fig. 1. Study area (A): Digital Elevation Model (DEM) of Uttarakhand province showing the 2 sampling sites and climatic grid points. (B): DEM of study sites (Map plotting source: GeoMapApp v. 3.6.10). (C): The subsurface sampling site at Nachiketa (NAT) surrounded by broadleaved trees. (D): Broadleaved forests at NAT. (E): The 42 cm deep subsurface sedimentary profile collected from NAT. (F): Bhojbasa area in the Gangotri valley. (G): Bhojbasa kame terrace (KMT), subsurface sampling site (H): The 105 cm deep subsurface sedimentary section collected from KMT.

University of East Anglia (CRU TS v. 3.23; (0.5 × 0.5°) grid; (Harris and Jones, 2015)) Figure 2. NAT area at temperate altitude of ~2,500 masl, receives an annual precipitation of ~1,100 mm. The alpine KMT site at 4,000 masl in the Gangotri valley receives relatively less annual precipitation, ~870 mm/yr, due to sharp right angle turn of the valley to the advancing direction of monsoon front (Sharma and Owen, 1996). The contribution ~76% (at NAT) and ~71% (at KMT) of annual rainfall in the summer months (June, July, August and September) indicates that ISM has dominant influence at the study sites. July remains the wettest month (~290 mm at NAT and ~215 mm at KMT) of the year. Winter months (December, January and February) contribute only around 10% (NAT) and ~12% (KMT) of the total rainfall. November remains the driest month with ~9 mm (NAT) and ~10 mm (KMT) rainfall. The mean annual temperature (MAT) for the areas are ~13.5 °C (NAT) and ~7.7 °C (KMT) with the highest temperature month of June (19.6 °C) for NAT and July (14.4 °C) for KMT, and the lowest in January (5.2 °C, NAT and −0.7 °C, KMT).

Both the study sites vary in their vegetation diversity and distribution according to precipitation (Fig. 1C–H). NAT (~2,500 masl), characterized by a small lake named Nachiketa Tal, has temperate type of vegetation with the dominance of broadleaved tree taxa, mainly *Quercus leucotricophora, Quercus floribunda, Alnus nepalensis, Juglans regia, Corylus jacquemontii, Carpinus viminea, Rhododendron arboreum, Ulmus wallichiana* etc. The Nachiketa sampling site is nearly devoid of conifers except for *Pinus roxburghii,* which grows dominantly on the comparatively drier open slopes at around 1 km aerial distance from the broadleaved forest range. Ground taxa families include Poaceae, Cyperaceae, Asteraceae, Ranunculaceae, Caryophyllaceae, Apiaceae, Geraniaceae, Caprifoliaceae, Amaranthaceae, Polygonaceae, etc. Ferns grow at the shady places under the canopy and at the moist pockets along the valley slopes. The site KMT (~4,000 masl) is a small meadow on the top of right lateral moraine near Bhojbasa (~3,800 masl) in the Gangotri Glacial valley. Gangotri glacier is one of the largest valley glaciers having 30 km length and width range of 0.5–2.5 km with area of 143 km^2, and the source of River Bhagirathi originating from glacier snout called as Gaumukh at ~3,900 masl (Singh et al., 2017). In the valley the tree-line is formed by the broadleaf arboreal *Betula utilis* at altitude ~3,800 masl near Bhojbasa, (~4 km downstream from the present glacier snout position). *Pinus wallichiana* (conifer) forms the upper growth limit at altitude ~3,700 masl near Chirbasa at ~9 km downstream from the present glacier snout position. The sub-alpine and alpine area in the valley are dominated by species of *Juniperus, Ephedra, Salix* and members of Cyperaceae, Asteraceae, Rosaceae, Brassicaceae, Ranunculaceae, Saxifragaceae and Polygonaceae (Kar et al., 2002). The temperate conifers (*Cedrus deodara, Picea smithiana* and *Abies pindrow*) and broadleaved trees (*Rhododendron arboreum, Quercus* spp.*, Alnus nepalensis, Corylus jacquemontii, Carpinus viminea, Ulmus wallichiana, Juglans regia* etc.) form their growth limits at further lower altitudes.

3. Materials and methods

A 42 cm deep sedimentary core was extracted from the temperate altitude of ~2,500 masl amidst the broadleaved dominant forest at Nachiketa (NAT) (Fig. 1) and sub sampled at 2 cm bulk intervals for proxy analyses. Lithology consisted of fine sand and silty clay from 42 to 10 cm and humic clay from 10 cm upto the surface. Another subsurface sedimentary core of 105 cm was collected by trench method from Kame terrace (KMT) near Bhojbasa at ~4,000 masl and sub sampled at 5 cm bulk intervals. The lithology comprised of fine sand to silt from 105 cm to 70 cm with intermittent layers of gritty to fine sand. Between 70 cm and 5 cm the lithology was silty clay. Organically rich humus was present from 5 cm depth till surface. The sub sampled sediments were studied for palynology and magnetic susceptibility (χlf) for both the profiles and additionally $\delta^{13}C_{org}$ for the NAT profile to reconstruct the vegetation and climate.

3.1. Radiocarbon dating

To provide age to both the sedimentary profiles, three sediment samples from each profile were radiocarbon (^{14}C) dated by AMS method at Inter University Accelerator Centre (IUAC), New Delhi, India. The sediments were treated by the Acid-Base-Acid methods to get rid of the inorganic carbon and humic acid (Sharma et al., 2019). Around 2 g of dried sediments were treated with 0.5 M Hydrochloric Acid (HCl) followed by 0.1 N Sodium Hydroxide (NaOH) on a thermostat shaker at 60 °C temperature and 650 rpm respectively for ten hours and three hours to dissolve the carbonates and humic acid. After each step of acid and alkali treatment the sediments were washed with mili-Q water to neutralize. The treated sediments were graphitized and measured for the ^{14}C signals by running them into the accelerated mass spectrometer (Kumar et al., 2015). The ^{14}C (AMS) dates obtained at different depths were calibrated using BACON program v. 2.4.3 (Blaauw and Christen, 2013) in 'R' language (Tables 1A and 1B) and the age-depth curve was plotted for both the sedimentary profiles (Fig. 3A and B).

3.2. Palynological processing

The pollen and spores were extracted from the sediment samples by

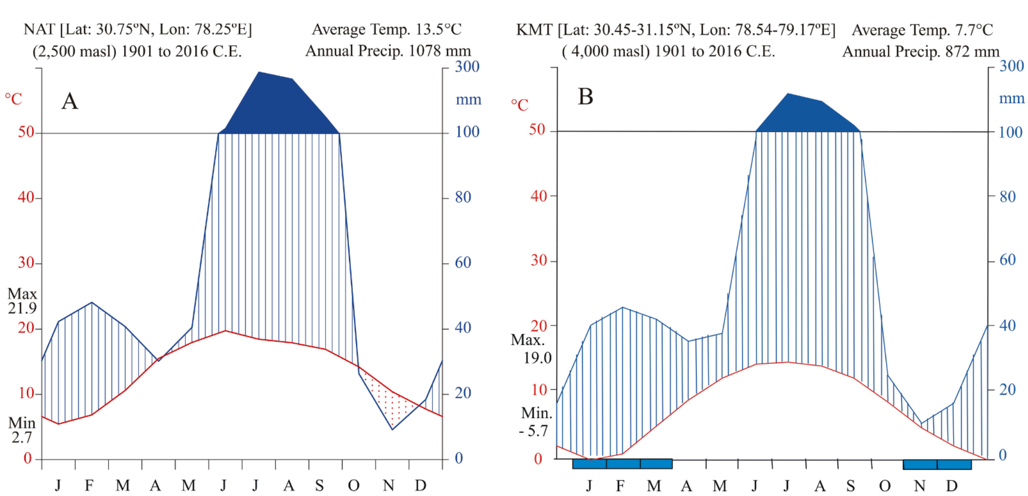

Fig. 2. The Walter-Leith climate diagrams showing temperature and precipitation values [CRU TS v. 3.22; (0.5x0.5°) data for the years 1901–2016 C.E.]. (A): Nachiketa (NAT) and (B): Gangotri (Bhojbasa kame terrace KMT).

Table 1A
^{14}C AMS dates along with the calibrated ages for Nachiketa (NAT) samples. *Calibrated ages are provide as 'ka BP' in the text (3300 cal yr BP = 3.3 ka BP)

Sample no.	Depth from surface (cm)	^{14}C Dates (yrs BP)	Calibrated ages (cal yr BP)*		Lab ID	$\delta^{13}C_{org}$ values (‰)
			μ	Σ		
1	6–8	369 ± 50	410	60	16C500	(−22.5) ± 0.2
2	20–22	681 ± 52	627	45	16C501	(−21.53) ± 0.2
3	38–40	2829 ± 55	2946	76	16C502	(−22.63) ± 0.2

Table 1B
^{14}C AMS dates along with the calibrated ages for Bhojbasa kame terrace (KMT) samples. *Calibrated ages are provide as 'ka BP' in the text (3300 cal yr BP = 3.3 ka BP)

Sample no.	Depth from surface (cm)	^{14}C Dates (yrs BP)	Calibrated ages (cal yr BP)*		Lab ID	$\delta^{13}C_{org}$ values (‰)
			μ	Σ		
1	15–17	274 ± 37	344	78	17C833	(−25) ± 2
2	55–60	IOM	—	—	17C834	—
3	78–82	3821 ± 47	4226	86	16C475	(−25) ± 2

IOM – Insufficient Organic Matter (less CO_2 = 126 μg; could not be processed).

following the standard maceration technique (Faegri and Iversen, 1989). About 25 g samples were initially treated with 36% of Hydrochloric Acid (HCl) to remove Calcium Carbonate ($CaCO_3$). The sediments were treated with 10% alkaline solution of Potassium Hydroxide (KOH) followed by 40% of Hydrofluoric Acid (HF) to remove humus and silica respectively. The samples were then acetolyzed with the acetolytic mixture (9:1 ratio of acetic anhydride and sulphuric acid) to dissolve cellulose (Erdtman, 1943), thus making the pollen-spores morphologically clear for identification. After every step of alkali and acid treatment the samples were washed thoroughly with distilled water. The macerals were stored in vial tubes in 50% glycerin. Macerals were studied for pollen identification and counting under the compound light microscope (Leica DM 2500). Relevant pollen keys (Demske et al., 2013; Gupta and Sharma, 1986; Moore et al., 1991) and pollen reference slides at the Birbal Sahni Institute of Palaeosciences (BSIP), Lucknow were used for the pollen identification. We counted 100–450 pollen-spores in each sample depending upon the enrichment of pollen-spores in the samples and considered the count as total palynomorph count (TPC). The pollen sum (PS) was calculated by excluding the counts of fern spores from TPC. Percentages of pollen were calculated on PS to enhance the frequency of recovered pollen taxa. The percentage of fern spores was calculated on TPC. Pollen diagrams Figure 4A, 4B, Supplementary Fig. S1 and Supplementary Fig. S2 were plotted using the software TILIA (Grimm, 2011) to represent changes in the percentages of pollen and spores. Few samples in both the profiles did not yield countable number of grains due to poor preservation of pollen-spores in the coarse sediments. However the few recovered pollen-spore grains in those samples were identified and marked as present (+) in the pollen diagrams. Variations in the calculated pollen percentages throughout the diagrams have been demarcated based on cluster analysis using the constrained incremental sum of squares (CONISS) method available in TILIA 1.7 software. Based on the demarcated variations in the percentages of pollen assemblages, each pollen diagram has been divided into different pollen zones representing the temporal vegetation changes.

3.3. Stable carbon isotope processing

For the isotopic studies ($\delta^{13}C_{org}$) of organic material, the sediments were air dried and ground into fine powder. Samples were treated with 5% HCl solution to eliminate the inorganic carbonates leaving only the organic carbon particles to be combusted in the reactor of Elemental Analyzer (Flash EA 2000) at BSIP, Lucknow. The treated samples along with known amounts of laboratory standards (IAEA CH_3, CH_6 and Sulfa) were packed in tin capsules and fed into the auto sampler of Elemental Analyzer (Flash EA 2000). The isotopic composition ($\delta^{13}C_{org}$) was calculated accordingly using the Continuous Flow Isotope Ratio Mass Spectrometer (CF-IRMS) coupled with ConFlow IV interface. The precision for the BSIP lab standards is ±0.1‰. The $\delta^{13}C_{org}$ data are expressed against Vienne Pee Dee Beleminite (VPDB).

3.4. Magnetic susceptibility measurements

The samples were dried at room temperature, crushed using agate pestle-mortar and noted amounts of samples packed tightly in the 10 cc plastic cuvettes after wrapping them in thin cling foil. The magnetic susceptibility of each sample was measured using the Bartington MS2B dual frequency susceptibility sensor. The readings for each sample were taken at low frequency (0.47 kHz) magnetic field (χlf). The calculations

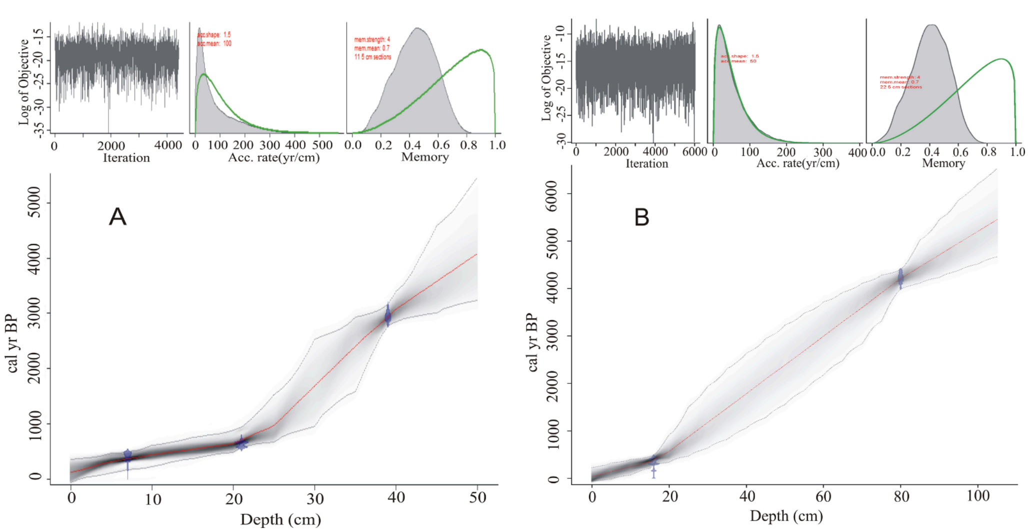

Fig. 3. Age-depth models of (A) 42 cm deep sedimentary profile (NAT) from Nachiketa site and (B) 105 cm deep sedimentary profile (KMT) from Gangotri Bhojbasa site using BACON program in 'R' language. KMT sample at the depth of 55–60 cm had insufficient organic carbon to date; so not included in the model.

are in SI system (m^3kg^{-1}). The data generation was done partly at the Indian Institute of Geomagnetism (IIG), Prayagraj, India and BSIP, Lucknow.

4. Results

4.1. Age-depth model

The subsurface sedimentary profile NAT covered the extrapolated time since ca. 3.3 ka BP till recent (Fig. 3A). The slow sedimentation rate (0.08 cm/decade) calculated the temporal resolution of ~256 years/sample between ca. 3.3 and 0.75 ka BP. The high (0.38 cm/decade) sedimentation rate provided the time resolution of ~52 years/sample since 0.75 ka till recent. The sedimentary profile KMT from Gangotri valley covered the time period since ca. 5 ka BP (extrapolated) till recent (Fig. 3B). In comparison to NAT sequence, the KMT sequence had faster sediment deposition rate that fluctuated from 0.18 to 0.5 cm/decade. The time resolution covered by each sample for this sequence is ~300 years between 4.2 and 0.4 ka BP, and ~125 years since 0.4 ka BP till recent.

4.2. Multiproxy analyses

The fluctuations in pollen percentages in both the sedimentary sequences are indicative of the vegetation and climate change Figure 4A, 4B, Supplementary Fig. S1 and Supplementary Fig. S2. Nachiketa (NAT) sequence from temperate meadow (Fig. 4A) recorded an overall high pollen frequency of *Pinus*, *Quercus* and *Alnus*. Ground vegetation majorly represented the pollen of Asteraceae (Liguliflorae, Tubuliflorae and *Artemisia*), Brassicaceae, Rosaceae, Caryophyllaceae, Ranunculaceae, Cyperaceae, Geraniaceae, Apiaceae, Polygonaceae and Pteridophytic spores. The $\delta^{13}C_{org}$ values fluctuated between −21.5‰ and −24.5‰ throughout the sequence. Magnetic susceptibility (χlf) values gradually changed from $97*10^{-8}$ m^3kg^{-1} at 3.3 ka BP to $30*10^{-8}$ m^3kg^{-1} during recent time. Pollen zone NAT-1 (42–29 cm depth; 3.3–1.5 ka BP) had low pollen counts with maximum of Geraniaceae pollen (29%) and fern spores (76% of TPC). $\delta^{13}C_{org}$ remained around –23‰ in this time. Pollen zone NAT-2 (29–19 cm depth; 1.5–0.6 ka BP) represented mainly the pollen of *Quercus* (24%), Cyperaceae (23%), *Pinus* (15%), Amaranthaceae (11%), *Alnus* (8%), *Betula* (2%) and *Carpinus* (2%). Caryophyllaceae pollen (2%) appeared at ca. 0.7 ka BP and existed till recent. The $\delta^{13}C_{org}$ value was −21.6‰ with a notable increase in the pollen percentages of Amaranthaceae and Asteraceae elements ca. 0.8 ka BP. Pollen zone NAT-3, (19–5 cm depth; 0.6 to 0.3 ka BP) had high pollen percentages of steppe taxa (34%) comprising Amaranthaceae, *Artemisia* and Asteraceae. between ~0.55 and 0.35 ka BP, the Amaranthaceae pollen (45%) became dominant and $\delta^{13}C_{org}$ (−21.8‰) value was also high. Fern spores (35% of TPC) declined during the time but Cyperaceae pollen (~22%) remained consistent. *Pinus* pollen increased in percentage since ca. 0.4 ka BP while *Quercus* pollen declined in frequency. Pollen zone NAT-4 (5 cm to surface; 0.3 ka BP till recent) had the dominance of *Pinus* (87%) pollen over *Quercus* (5%), and decrease in $\delta^{13}C_{org}$ value (−24.5‰).

Pollen assemblage of Kame terrace (KMT) sequence (Fig. 4B) in the Gangotri valley recovered the dominance of non-arboreal pollen (steppe elements, Rosaceae, Ranunculaceae, Caryophyllaceae, Saxifragaceae, Cyperaceae and Poaceae) over arboreal pollen (*Pinus, Cedrus, Betula, Quercus, Alnus* etc.). The χlf values fluctuated between $3*10^{-8}$ m^3kg^{-1} and $10*10^{-8}$ m^3kg^{-1}. Pollen zone KMT-1 (105–85 cm depth; ~5–4.4 ka BP) had pollen dominance of Liguliflorae (20%), Cyperaceae (15%), Geraniaceae (10%), Tubuliflorae (10%), Poaceae (6%) and Caryophyllaceae (5%). Pollen Zone KMT-2 (85–70 cm; 4.4–3.6 ka BP) had dominant pollen frequency of Cyperaceae (48%) and steppe elements (33%). The latter includes Liguliflorae (23%), Tubuliflorae (7%) and *Artemisia* (2%). In the pollen Zone KMT-3 (70–35 cm; 3.6–1.5 ka BP) the pollen frequency of Cyperaceae (64%) increased. Pollen of Poaceae (4%), Asteraceae, *Thalictrum* and other Ranunculaceae (3% each) were significantly present. Moreover there was an increase in the pollen assemblage of steppe elements (10%) ca. 2.9–2.5 ka BP. Pollen Zone KMT-4 (35–15 cm; 1.5–0.4 ka BP) also had dominance of Cyperaceae (54%) over Poaceae (6%), *Thalictrum* (5%), *Abies* (4%), *Artemisia* (4%), Tubuliflorae (3%) and Ranunculaceae (3%). Pollen Zone KMT-5 (15 cm

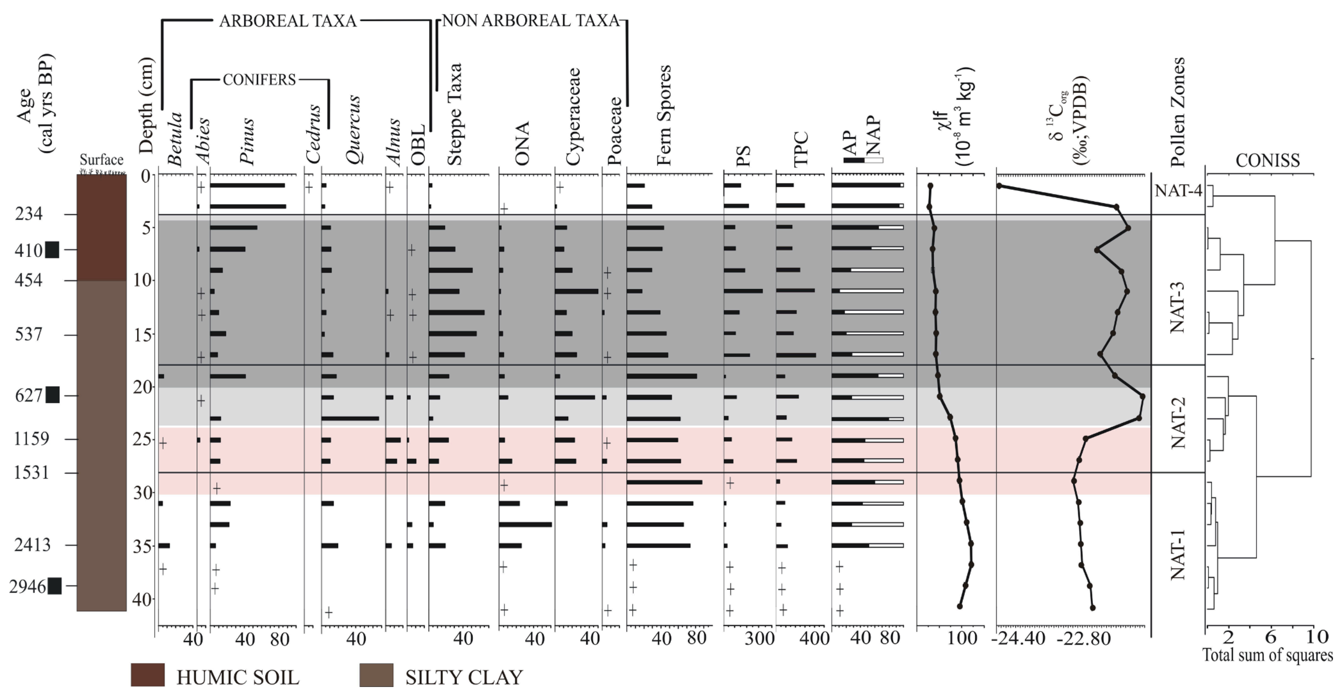

Fig. 4A. Composite diagram of the 42 cm deep sedimentary profile from Nachiketa (NAT). '+' = <1%. OBL = Other broadleaved taxa. ONA = Other nonarboreal taxa. AP = Arboreal pollen. NAP = Nonarboreal pollen. TPC = Total Palynomorph Counts. PS = Pollen Sum. Grey band indicates dry climatic phase; darker grey band indicates drier conditions. Pink band indicates moist MWP. (For interpretation of the references to colour in this figure legend, the reader is referred to the web version of this article.)

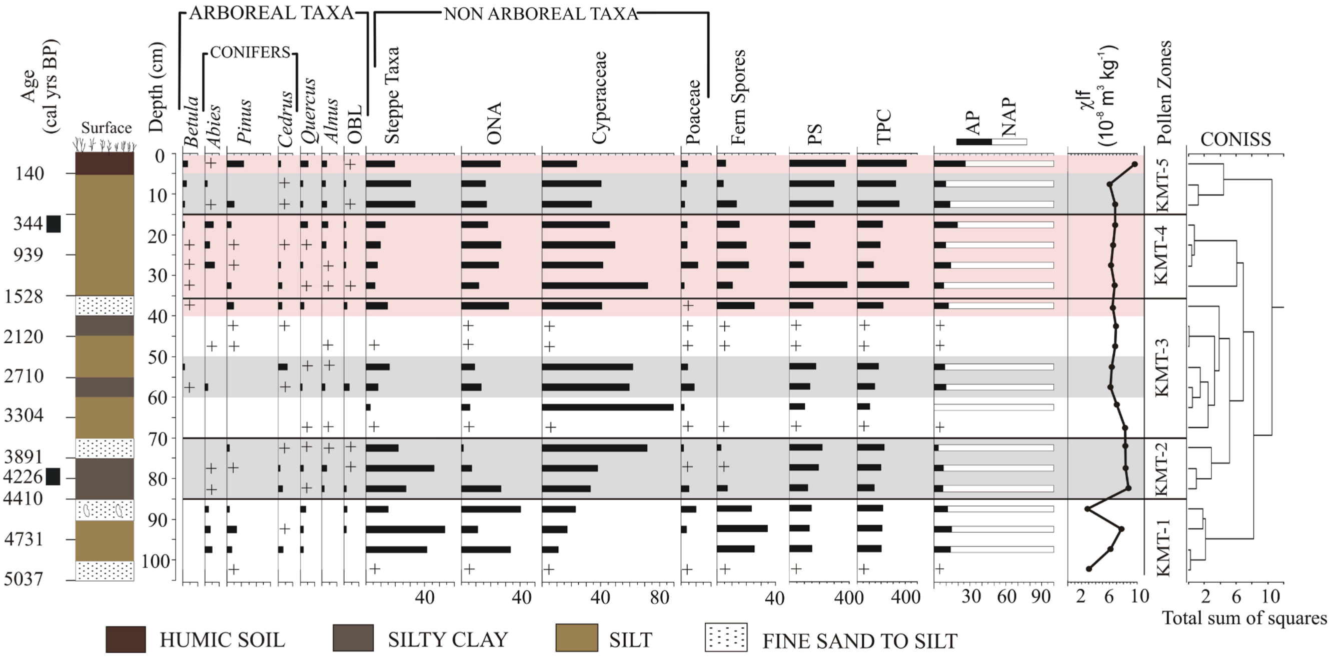

Fig. 4B. Composite diagram of the 105 cm deep sedimentary profile from Gangotri Bhojbasa (KMT). '+' = <1%. OBL = Other broadleaved taxa. ONA = Other nonarboreal taxa. AP = Arboreal pollen. NAP = Nonarboreal pollen. TPC = Total Palynomorph Counts. PS = Pollen Sum. Grey band indicates dry climatic phase. Pink band indicates moist MWP.

to surface; 0.4 ka BP till recent) had good representation of Cyperaceae (33%). Pollen of Liguliflorae (10%), Tubuliflorae (9%), *Pinus* (7%), *Artemisia* (6%), Rosaceae (5%), *Quercus*, *Alnus*, Poaceae and Saxifragaceae (3% each) were also significantly present.

The demarcated zones in pollen diagrams of both the study sites (NAT and KMT) representing the temporal changes in the pollen assemblages and other proxy parameters (χlf and $\delta^{13}C_{org}$) have been elaborated further in the supplementary file.

5. Discussion

Sedimentary archives have often been analyzed to interpret the palaeoclimatic fluctuations both regionally and locally (Bhattacharyya, 1989; Chakraborty et al., 2006; Kar et al., 2002; Leipe et al., 2014; Rawat et al., 2015; Singh et al., 2021). Here we have evaluated and compared the vegetation data from two neighboring valleys but having different mean annual precipitations. The pollen counts for both the profile were low due to the silty-sandy nature of the sedimentary profiles. But based on the fluctuations in the recovered pollen assemblage and $\delta^{13}C_{org}$ values, we were able to record the major and short-lived climatic events of late Holocene time. The gradual decline in the χlf values suggested a continuous infilling of the meadows during the late Holocene time under low energy fluvio-lacustrine depositional environment (Wan et al., 2004; Sandeep et al., 2017; Lone et al., 2020).

5.1. Hydroclimatic signals corresponding to the 4.2 ka event

The subsurface profile KMT from Gangotri valley dated back to ca. 5 ka BP and recovered high percentage of steppe elements between ca. 4.8 and 3.5 ka BP (Fig. 5). The percentage was even higher between ca. 4.4 and 3.8 ka BP correlating with the dry 4.2 ka event reported globally (Kaniewski et al., 2018). Relative increase in percentage of Rosaceae pollen and significant decline of *Pinus* and *Abies* pollen and fern spores signify the dry conditions during this time. Lack of high resolution database in a previous study from the same Gangotri valley (Ranhotra et al., 2001) could not report this dry event from the valley. Impact of this event was also addressed from the neighboring Dokriani valley,

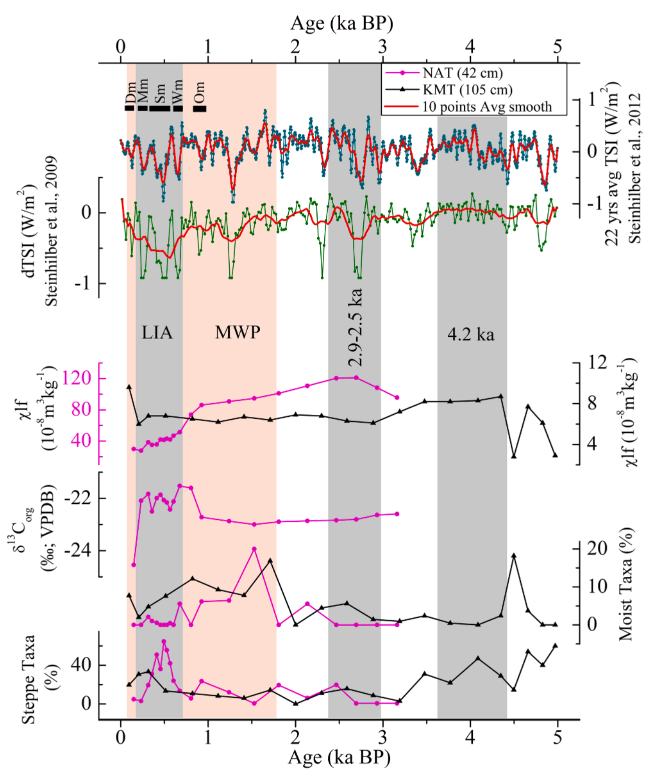

Fig. 5. Comparison of various proxy data of both studied profiles with TSI and sunspot minima activities: Oort (Om), Wolf (Wm), Spörer (Sm), Maunder (Mm) and Dalton (Dm) since ca. 5 ka BP. The grey bands indicate dry climatic phase and pink band indicates moist MWP. Avg = Average. (For interpretation of the references to colour in this figure legend, the reader is referred to the web version of this article.)

which revealed diminished retreat rate of Dokriani glacier snout between 4.3 and 3.7 ka (Shukla et al., 2018). Phadtare (2000) also reported a marked decline in the summer monsoon strength between 4 ka and 3.5 ka by analyzing peat deposits of Dokriani valley. An abrupt shift in $\delta^{18}O$ data from the speleothems of Mawmluh Cave, in Meghalaya province (Berkelhammer et al., 2012; Fig. 6) was recorded ca. 4.2 ka based on which the Meghalayan age was designated in the Holocene epoch (Walker et al., 2012, 2018, 2019). However there is an observed variation in the time periods of this wide spread aridity phase as reported from different regions of Himalaya. In the northwest part a 're-turn of permafrost' was reported from Ladakh at ca. 4.2 ka based on pollen-spore and geochemical datasets (Wünnemann et al., 2010). This correlates well to the cool-dry phase recorded ca. 4.2 ka in the Guliya ice core from Tibet (Thompson et al., 1997; Fig. 6). Demske et al. (2009) reported an abrupt shift towards aridity in the TsoKar region of Ladakh, Trans-Himalaya, ca. 4.8 ka based on pollen evidences of an expansion of Chenopodiaceae-dominated desert-steppe. The subsequent pollen record and moisture reconstructions from Tso Moriri, Ladakh (Leipe et al., 2014) suggested prolonged Holocene trend towards aridity from ca. 5.2 to 3 ka punctuated by an interval of increased dryness between ca. 4.5 and 3.6 ka and ca. 3.2 ka. These dry phases might have pushed the Harappan culture to develop more efficient agricultural practices and to deal with water shortages. In the western part of Himalaya, Rawat et al. (2015) recorded an intermittent cold and dry spell between ca. 4.8 ka and 4.3 ka by analyzing pollen from the Chandra Taal at Lahaul-Spiti, Himachal Pradesh (Fig. 6). The time period of this dry spell also coincided with the findings from Ladakh (Demske et al., 2009). Kinnaur region in Himachal Pradesh province too experienced a weaker monsoonal phase between ca. 4.8 ka and 2 ka (Chakraborty et al., 2006).

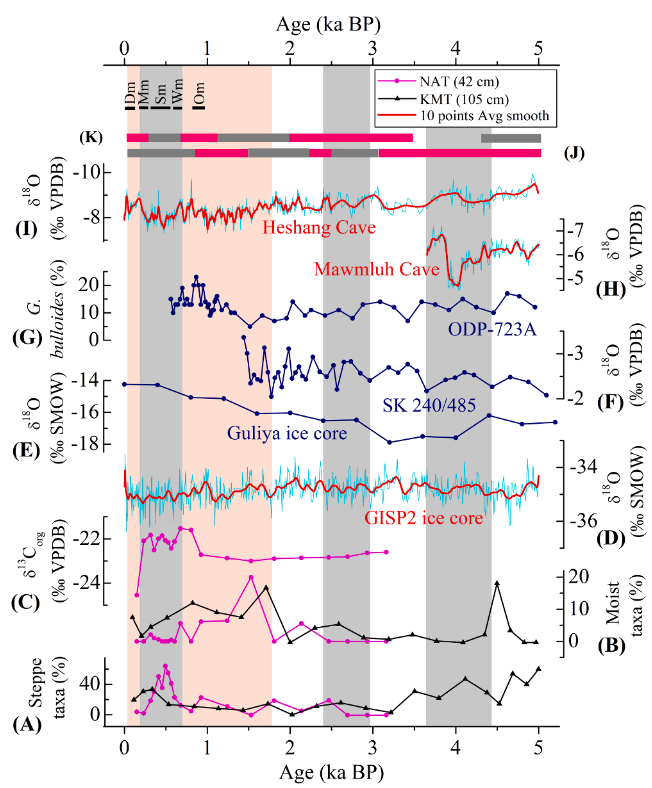

Fig. 6. Comparison of various proxy data of both studied profiles (A–C) with ice core data: (D) Grootes and Stuiver, 1997; (E) Thompson et al., 1997; marine data: (F) Azharuddin et al., 2017; (G) Gupta et al., 2003; $\delta^{18}O$ speleothem: (H) Berkelhammer et al., 2012; (I) Hu et al., 2008; lacustrine deposits (grey is for dry and pink is for moist): (J) Srivastava et al., 2017; (K) Rawat et al., 2015. Avg = Average. The grey bands indicate dry climatic phase and pink band indicates moist phase. (For interpretation of the references to colour in this figure legend, the reader is referred to the web version of this article.)

However poor sample resolution and age constrains could not resolve the climatic events at finer temporal resolution. From the ISM dominant regions of Uttarakhand Himalaya, an overall cool phase was experienced with warm and wet intervals between 5.4 ka and 3.8 ka from the Kedarnath valley with moderate monsoon between 4.8 ka and 3.2 ka (Srivastava et al., 2017; Fig. 6). A cool-dry phase between 4 ka and 3.5 ka was also discussed by analyzing the lake sediments from western Himalaya (Chauhan and Sharma, 1996; Kotlia et al., 1997), Lonar Lake in Indian tropical core-monsoon zone (Anoop et al., 2013; Prasad et al., 2014), and even based on *G. bulloides* and *G. ruber* records from the Arabian Sea (Azharuddin et al., 2017; Gupta et al., 2003; Fig. 6). A recent finding from the Gangetic Plains (Singh et al., 2021) reported an overall transition towards dry phase since ca. 5.8 ka BP that further intensified between ca. 4.2 and 4.0 ka. The 4.2 ka event, also assigned as the 'Holocene turnover' (Paasche et al., 2004) or 'Neoglaciation' (Denton and Karlén, 1973), that occurred due to the reduced summer insolation with a drop in temperature at the Northern Hemisphere. In our study as well the low and high pollen frequency of respective moist and steppe taxa recorded in the KMT sequence, corresponded with the reduced summer insolation (Steinhilber et al., 2009, 2012; Fig. 5). The speleothem $\delta^{18}O$ records from the Sahiya Cave located in the ISM dominated part of the Uttarakhand province (Kathayat et al., 2017) recovered a long-term decline in ISM precipitation. The decreasing Northern Hemisphere summer insolation and a southward migration of the ITCZ over the past 5.7 ka BP were discussed as the factors. Contrarily, Kathayat et al. (2018) based on speleothem $\delta^{18}O$ record from the Mawmluh Cave concluded the presence of a wetter phase amidst 2 multi-decadal droughts between 4.2 ka and 3.9 ka BP. Ran and Chen (2019) also conferred that while the 4.2 ka BP event was a drier period, a different climate pattern emerged in the central-southern Levant and Dead Sea area. This climate pattern showed two arid phases suggesting a 'W-shaped event' framing-in a wetter period. An abrupt 4‰ increase in $\delta^{18}O$ of gastropod aragonite from sediments of palaeolake Kotla Dahar in Haryana province occurred at ca. 4.1 ka, deducing a sharp reduction in ISM intensity (Dixit et al., 2014), caused by changes in the Indian Ocean Dipole (IOD) and El Niño Southern Oscillation (ENSO) (Fisher et al., 2008; MacDonald, 2011). Few workers also argued that the changes in the direction and intensity of the cyclonic North Atlantic westerlies, controlled by the North Atlantic Oscillation (NAO), resulted to 4.2 ka BP event (Kaniewski et al., 2018). However, the driving mechanism behind this intense arid phase is yet debatable. Walker et al. (2018) believed for no evidence of massive fresh water release into the North Atlantic, and also there were no major changes in the corresponding solar activity (Gupta et al., 2003). The recorded widespread cold-arid phase between ca. 4.8 ka and 3.5 ka in South Asian region coincide with the Bond cold event 3 of the North Atlantic (Bond et al., 2001) and seemed to be a long term drying trend instead of an abrupt 4.2 ka cooling. Holocene climate study from Lonar Lake in central India (Prasad et al., 2014) discussed that the aridity started earlier and intensified ca. 4.2 ka. This event being a gradual climate shift rather than an abrupt shift has also been highlighted by other regional records (Arz et al., 2006). The 4.2 ka cold-dry event has been observed as a global phenomenon of decreased monsoon precipitation causing severe droughts (Gasse, 2000; Staubwasser et al., 2002). This dry event resulted in the decline of many cultures and civilizations, such as Harappan culture of the Indus valley civilization (Dixit et al., 2014), Akkadian Empire in Mesopotamia (Cullen et al., 2000), end of the Egyptian Kingdom due to reduction in the Nile river flow (Marshall et al., 2011) and the Longshan culture in China (Chang, 1999; Liu and Feng, 2012). Ran and Chen (2019) deliberated that the fall down of nearly all well-developed Neolithic cultures at ~4.2 ka BP though correlated with the 4.2 ka climate anomaly, but either drying and/or cooling at ~4.2 ka might not be sufficient to collapse these well-developed cultures. This therefore needs further investigations to constrain the 4.2 ka climatic and environmental variables.

5.2. Hydroclimatic signals corresponding to the MWP and LIA

There is an observed increase in the frequency of few steppe elements between ca. 2.9 and 2.5 ka BP in the KMT sequence from Gangotri valley and ca. 2.4 ka BP in the NAT sequence that nearly coincides with the low TSI (Fig. 5). This suggested an intermittent dry phase indicating decline of ISM precipitation in the area. The dry phase ca. 2.8 ka has been evidenced from few other regions in the Northern Hemisphere (Dzięgielewskia et al., 2013; Klimenko, 2004). Decline in the $\delta^{18}O$ values from the Greenland ice core GISP2 (Stuiver et al., 1995; Fig. 6) was recorded ca. 2.9–2.7 ka and relates well with the drop in TSI during this time. Low pollen influx values were registered ca. 2.8–1.3 ka at Tso-Kar region of Ladakh (Demske et al., 2009) suggesting less vegetation cover. Since ca. 1.8 ka BP our study sites recorded enhancement in the growth of conifers (*Pinus, Abies, Cedrus*), temperate broadleaved taxa (*Quercus, Betula, Corylus, Alnus*) and non-arboreal vegetation assemblage (Ranunculaceae, *Thalictrum*, Geraniaceae, Polygonaceae etc.) indicating increase in moist conditions. The warm-moist conditions intensified ca. 1.5 ka BP as inferred by the high pollen assemblage of moist taxa at both the study sites and the low $\delta^{13}C_{org}$ values in the NAT sequence (Fig. 5). The moist phase between 1.5 and 0.9 ka BP (450–1050 C.E.) was linked to the enhanced ISM precipitation that also bracketed the medieval warm period (MWP) identified around 900–1300 C.E. over northern hemisphere (Graham et al., 2011).

An increase in pollen frequency of steppe taxa, mainly Amaranthaceae at NAT and Asteraceae (Liguliflorae, Tubuliflorae, *Artemisia*), *Ephedra* and Saxifragaceae at KMT site, was noticed since ca. 0.8 ka BP Figure 5, Supplementary Fig. S1 and Supplementary Fig. S2. This indicated decline of ISM intensity in the region. The dryness further intensified ca. 0.6 ka BP with observed peaks in the steppe pollen assemblage between 0.6 and 0.3 ka BP (1350–1650 C.E.) at NAT site and between 0.5 and 0.2 ka BP (1450–1750 C.E) at KMT site. This dry phase well corresponded with the Little ice age (LIA) cool event prominent over the northern hemisphere (Mann, 2002). The reconstructed hydroclimatic conditions of our study also corresponded with some of the available pollen and $\delta^{13}C$ based climate records (Ali et al., 2018; Bhattacharyya, 1989; Chakraborty et al., 2006; Srivastava et al., 2017; Trivedi et al., 2011) as shown in Fig. 6. Palynological data from the adjacent Dokriani valley (Phadtare, 2000) and Gangotri valley (Kar et al., 2002) indicated warm-moist conditions ca. 1.8–0.8 ka BP and cool-dry phase till ca. 0.2 ka BP. Brief moist climatic conditions between 2 ka and 1 ka were also observed from the speleothem $\delta^{18}O$ records of Siddha Baba Cave (Denniston et al., 2000), Sahiya Cave (Kathayat et al., 2017) and Heshang Cave (Hu et al., 2008; Fig. 6). Recent study on tree-ring chronology of *Juniperus* from Lahaul-Spiti by Managave et al. (2020) showed warm and dry conditions prior to 1300 C.E. that changed to cool-wet from ca. 1300 to 1560 C.E. and ca. 1650 to 1800 C.E. Rowan (2017) too demonstrated the expansion of Himalayan glaciers between 1300 and 1600 C.E. that also matches the period of strong WDs. Strong WD during the LIA has also been discussed from the cave deposits located in the ISM dominant regions of western Himalaya (Kotlia et al., 2015, 2017; Liang et al., 2015; Sanwal et al., 2013). However, a recent glacier mass balance (GMB) reconstruction (Shekhar et al., 2017) using tree-rings chronology of *Abies* and *Pinus* revealed that most of the western Himalayan glaciers experienced negative mass balance in the Himalayan region during the latter phase of LIA that is after ca. 1600 C.E.

MWP and LIA were more distinct in the Northern Hemisphere than the Southern Hemisphere especially for the extra-tropics (Mann et al., 2009). La-Nina like pattern in the tropical Pacific brought warmth in the North Pacific (Mann et al., 2009) resulting in a near 1 °C warmer sea-surface temperature during the MWP than today (Keigwin, 1996). The interval between 950 and 1250 C.E. was observed as a strong monsoon period not only in the Lesser Himalaya and Central India, but also in the Arabian Sea records (Sinha et al., 2011a, 2011b). Nevertheless, there were signatures of major drought between 1300 and 1350 C.E. in the Andamans (Laskar et al., 2013), and in marine record from Arabian Sea (Gupta et al., 2003; Tiwari et al., 2006). Subsequently, the temperature of the Northern Hemisphere dropped by about 0.6 °C during the 15th to 19th centuries (LIA) outside the North Atlantic region as well (Mann, 2002) when the SST was 1 °C cooler than today (Keigwin, 1996). The LIA period was the resultant of low ISM precipitation which in turn led to stronger WD.

In our record the dry phases with the high values of steppe pollen assemblages and high $\delta^{13}C_{org}$ values between 1350 and 1750 C.E. reflected the weak ISM. These dry phases also corresponded with the low TSI values where the sunspot activity was minimum (Fig. 5). However, during LIA phase, there was an observed inconsistency amongst the time frames of the peaks of steppe pollen assemblage from both the sites (Fig. 5). At the temperate altitude site NAT, the steppe pollen assemblage showed highest value peak between ca. 0.6 and 0.3 ka BP (1350–1650 C.E.). In contrast, the steppe pollen assemblage from alpine meadow site KMT in Gangotri valley showed high values between 0.5 and 0.2 ka BP (1450 and 1750 C.E.). This centennial scale temporal inconsistency amongst the steppe and moist pollen assemblages from the two sites could be a response of site location towards the summer monsoon. Site NAT is located at the temperate altitude and receive high amount of summer precipitation. Site KMT, located at the alpine altitude, is away from the summer monsoon front and receives comparatively less precipitation during summer monsoon months (JJAS) with extended days of winter snow through WD. In the latter phase of LIA, i.e. after ~1600 C.E., the northward migratory phase of ITCZ resulted to weakening of WD strength. The influence of weakening WD might have started earlier at the ISM dominant temperate altitudes of lesser Himalaya than at greater and trans-Himalayan regions. The post 1600 C.E. negative mass balance of western Himalayan glaciers (Shekhar et al., 2017) also support the weak effect of LIA, mainly in the ISM dominant regions. The oxygen isotope composition of the stalagmites from cave sites Sainji (Kotlia et al., 2015) and Panigarh (Liang et al., 2015), situated at the northern margin of the present day summer ITCZ, showed prominent variations attributed to changes in the ISM strength and seasonal precipitation induced by the migration of the ITCZ (Dimri et al., 2016). However, in our study, the difference in the temporal resolution of samples from both the sites and influence of localized topographical and environmental factors cannot be ruled out. More precise understanding of this behavioral pattern and connectivity between the ITCZ and winter westerly is needed. This is possible only by augmenting the existing knowledge with the climate reconstructions of high temporal resolution from different precipitation regimes of the Himalayan region.

6. Conclusions

The proxy data analyses of subsurface sedimentary sequences from the meadow sites, located at temperate and alpine altitudes in the ISM dominated region of western Himalaya, provided the climatic variations in the region for past 5 ka. We recorded a weak ISM phase between 4.4 and 3.8 ka BP from the alpine area within the Gangotri valley that corresponded with the 4.2 ka BP cool-arid global event. The 4.2 ka event is otherwise poorly documented from the monsoon dominant regions of Himalaya through palynological records, either due to age constraints or analyses of low temporal resolution archives. The intermittent ISM decline between ca. 2.9 and 2.5 ka BP was weakly observed from the studied sites. This might be attributed to low temporal resolution of samples thus diluting the signals. The reported strong (weak) ISM precipitation ca. 1.5 to 0.9 ka BP (0.6 to 0.2 ka) by the palynological and $\delta^{13}C_{org}$ records coincide well with the time-periods of globally known MWP (LIA) climate anomalies. The recovered late Holocene strong (weak) ISM phases from both the sites correspond with the high (low) solar irradiance and accord with the climatic anomalies recorded from the north Atlantic region and other higher latitudes. This explained the teleconnection of south Asian monsoonal dynamics with the climate circulations over the north Atlantic region, mainly driven by the changes in solar insolation. Moreover, during the LIA, there was an observed temporal inconsistency of a centennial scale amongst the palynological data derived from the two sites which receive variable amount of ISM precipitation. We could assess that after ca. 1600 C.E. the influence of LIA started weakening earlier at the ISM dominant southern parts of western Himalaya than the WD influenced northern parts of the western Himalaya. This study has provided a perception to further explore the dynamics of summer and winter monsoon circulations by assessing the sensitivity of biotic and abiotic proxies to monsoon systems across the Himalayan region.

CRediT authorship contribution statement

Ipsita Roy: Conceptualization, Methodology, Formal analysis, Investigation, Writing – original draft, Visualization. **Parminder Singh Ranhotra:** Conceptualization, Validation, Resources, Writing – review & editing, Supervision, Project administration, Funding acquisition. **Nidhi Tomar:** Methodology, Investigation, Visualization. **Mayank Shekhar:** Software, Resources. **Shailesh Agrawal:** Formal analysis, Resources. **Amalava Bhattacharyya:** Methodology. **Pankaj Kumar:** Formal analysis, Resources. **Shiva Kumar Patil:** Formal analysis, Resources. **Rajveer Sharma:** Formal analysis.

Declaration of Competing Interest

The authors declare that they have no known competing financial interests or personal relationships that could have appeared to influence the work reported in this paper.

Acknowledgements

The authors are indebted to the Director, Birbal Sahni Institute of Palaeosciences (BSIP), Lucknow for permission to carry out this work and for publication (BSIP/RDCC/ Publication No. 97/2020-21) and inhouse project 5.8 funding. PSR is thankful to the Science and Engineering Research Board (SERB), New Delhi for the financial support vide SERB-DST project No SR/DGH-56/2013. IR is thankful to DST-INSPIRE (IF150998) for funding her fellowship during the preparation of this manuscript. Thanks are highly due to the Uttarakhand forest department and forest officials (PCCF, Uttarakhand and DFO Uttarkashi) and to Mrs. Meenakshi Joshi (IFS) for kind permission and support in the field work. We are grateful to the Director, Inter-University Acceleration Center (IUAC), New Delhi, for providing infrastructure and instrument facility to get the AMS dates. We thank Directors, KSKGRL, Indian Institute of Geomagnetism, Prayagraj and BSIP, Lucknow for facilities to carryout magnetic susceptibility measurements.

Appendix A. Supplementary material

Supplementary data to this article can be found online at https://doi.org/10.1016/j.jseaes.2022.105080.

References

Ali, S.N., Dubey, J., Ghosh, R., Quamar, M.F., Sharma, A., Morthekai, P., Dimri, A.P., Shekhar, M., Arif, M., Agrawal, S., 2018. High frequency abrupt shifts in the Indian summer monsoon since Younger Dryas in the Himalaya. Sci. Rep. 8, 1–8.

Anoop, A., Prasad, S., Plessen, B., Basavaiah, N., Gaye, B., Naumann, R., Menzel, P., Weise, S., Brauer, A., 2013. Palaeoenvironmental implications of evaporative gaylussite crystals from Lonar Lake, central India. J. Quat. Sci. 28 (4), 349–359.

Arz, H.W., Lamy, F., Pätzold, J., 2006. A pronounced dry event recorded around 4.2 ka in brine sediments from the northern Red Sea. Quat. Res. 66, 432–441.

Azharuddin, S., Govil, P., Singh, A.D., Mishra, R., Agrawal, S., Tiwari, A.K., Kumar, K., 2017. Monsoon-influenced variations in productivity and lithogenic flux along offshore Saurashtra, NE Arabian Sea during the Holocene and Younger Dryas: A multi-proxy approach. Palaeogeogr. Palaeoclimatol. Palaeoecol. 483, 136–146.

Berger, A., Loutre, M.F., 1999. Parameters of the Earth's orbit for the last 5 Million years in 1 kyr resolution. PANGAEA. 10.1594/PANGAEA.

Berkelhammer, M., Sinha, A., Stott, L., Cheng, H., Pausata, F.S., Yoshimura, K., 2012. An abrupt shift in the Indian monsoon 4000 years ago. Geophys. Monogr. Ser. 198, 75–87.

Bhattacharyya, A., 1989. Vegetation and climate during the last 30,000 years in Ladakh. Palaeogeogr. Palaeoclimatol. Palaeoecol. 73 (1-2), 25–38.

Bhattacharyya, A., Ranhotra, P.S., Gergan, J.T., 2011. Vegetation vis-a-vis climate and glacier history during 12,400 to 5,400 yr BP from Dokriani valley, Garhwal Himalaya, India. J. Geol. Soc. India 77, 401–408.

Blaauw, M., Christen, J.A., 2013. Bacon Manual e v2. 2. Blaauw, M., Wohlfarth, B., Christen, J.A., Ampel, L., Veres, D., Hughen, K.A., Preusser, F., et al. 2010. Were last glacial climate events simultaneous between Greenland and France, pp. 387–394.

Bond, G., Kromer, B., Beer, J., Muscheler, R., Evans, M.N., Showers, W., Hoffmann, S., Lotti-Bond, R., Hajdas, I., Bonani, G., 2001. Persistent solar influence on North Atlantic climate during the Holocene. Science 294 (5549), 2130–2136.

Booth, R.K., Jackson, S.T., Forman, S.L., Kutzbach, J.E., Bettis, E.A., Kreigs, J., Wright, D. K., 2005. A severe centennial-scale drought in midcontinental North America 4200 years ago and apparent global linkages. The Holocene 15 (3), 321–328.

Bradley, R.S., Hughes, M.K., Diaz, H.F., 2003. Climate in medieval time. Science 302 (5644), 404–405.

Chakraborty, S., Bhattacharya, S.K., Ranhotra, P.S., Bhattacharyya, A., Bhushan, R., 2006. Palaeoclimatic scenario during Holocene around Sangla valley, Kinnaur northwest Himalaya based on multi proxy records. Curr. Sci. 91, 777–782.

Chang, K.C., 1999. China on the Eve of the Historical Period. The Cambridge history of ancient China: from the origins of civilization to 221, 37–73.

Chauhan, M.S., Sharma, C., 1996. Late Holocene vegetation of Darjeeling (Jore-Pokhari) eastern Himalaya. Palaeobotanist 45, 125–129.

Crowley, T.J., Lowery, T.S., 2000. How warm was the medieval warm period? AMBIO: J. Hum. Environ. 29 (1), 51–54.

Cullen, H.M., Demenocal, P.B., Hemming, S., Hemming, G., Brown, F.H., Guilderson, T., Sirocko, F., 2000. Climate change and the collapse of the Akkadian empire: Evidence from the deep sea. Geology 28, 379–382.

Demske, D., Tarasov, P.E., Nakagawa, T., 2013. Atlas of pollen, spores and further non-pollen palynomorphs recorded in the glacial-interglacial late Quaternary sediments of Lake Suigetsu, central Japan. Quat. Int. 290-291, 164–238.

Demske, D., Tarasov, P.E., Wünnemann, B., Riedel, F., 2009. Late glacial and Holocene vegetation, Indian monsoon and westerly circulation in the Trans-Himalaya recorded in the lacustrine pollen sequence from Tso Kar, Ladakh, NW India. Palaeogeogr. Palaeoclimatol. Palaeoecol. 279 (3-4), 172–185.

Denniston, R.F., González, L.A., Asmerom, Y., Sharma, R.H., Reagan, M.K., 2000. Speleothem evidence for changes in Indian summer monsoon precipitation over the last 2300 years. Quat. Res. 53 (2), 196–202.

Denton, G.H., Karlén, W., 1973. Holocene climatic variations—their pattern and possible cause. Quat. Res. 3 (2), 155–205.

Dimri, A.P., Mohanty, U.C., 2009. Simulation of mesoscale features associated with intense western disturbances over western Himalayas. Meteorol. Appl.: J. Forecast. Pract. Appl. Train. Tech. Modell. 16 (3), 289–308.

Dimri, A.P., Yasunari, T., Kotlia, B.S., Mohanty, U.C., Sikka, D.R., 2016. Indian winter monsoon: Present and past. Earth-Sci. Rev. 163, 297–322.

Dimri, A.P., Yasunari, T., Wiltshire, A., Kumar, P., Mathison, C., Ridley, J., Jacob, D., 2013. Application of regional climate models to the Indian winter monsoon over the western Himalayas. Sci. Total Environ. 468-469, S36–S47.

Dixit, Y., Hodell, D.A., Petrie, C.A., 2014. Abrupt weakening of the summer monsoon in northwest India~ 4100 yr ago. Geology 42, 339–342.

Draganits, E., Gier, S., Hofmann, C.-C., Janda, C., Bookhagen, B., Grasemann, B., 2014. Holocene versus modern catchment erosion rates at 300 MW Baspa II hydroelectric power plant (India, NW Himalaya). J. Asian Earth Sci. 90, 157–172.

Dzięgielewskia, K., Nalepkab, D., Walanusc, A., 2013. Dry swamp? Researching a peat bog and settlement in Podłęże near Kraków as a contribution to climate reconstruction in the early Subatlantic period. Archaeol. Polona 49.

Erdtman, G., 1943. An Introduction to Pollen Analysis. Waltham, Massachusetts, Chronica Botanica [2nd printing, 1954].

Faegri, K., Iversen, J., 1989. Textbook of Pollen Analysis, IV Edition. In: Faegri, K., Kaland, P.E., Krzywinski, K. (Eds.), Chichester. John Wiley & Sons, USA.

Fisher, D., Osterberg, E., Dyke, A., Dahl-Jensen, D., Demuth, M., Zdanowicz, C., Bourgeois, J., Koerner, R.M., Mayewski, P., Wake, C., Kreutz, K., Steig, E., Zheng, J., Yalcin, K., Goto-Azuma, K., Luckman, B., Rupper, S., 2008. The Mt Logan Holocene—late Wisconsinan isotope record: tropical Pacific—Yukon connections. The Holocene 18 (5), 667–677.

Gasse, F., 2000. Hydrological changes in the African tropics since the Last Glacial Maximum. Quat. Sci. Rev. 19 (1-5), 189–211.

Ghosh, R., Bera, S., Sarkar, A., Paruya, D.K., Yao, Y.-F., Li, C.-S., 2015. A~ 50 ka record of monsoonal variability in the Darjeeling foothill region, eastern Himalayas. Quat. Sci. Rev. 114, 100–115.

Graham, N.E., Ammann, C.M., Fleitmann, D., Cobb, K.M., Luterbacher, J., 2011. Support for global climate reorganization during the "Medieval Climate Anomaly". Clim. Dyn. 37 (5-6), 1217–1245.

Grimm, E.C. 2011. TILIA 1.7. 16. Illinois State Museum. Research and Collection Center, Springfield, USA.

Grootes, PM, Stuiver, M, 1997. Oxygen 18/16 variability in Greenland snow and ice with 10− 3-to 105-year time resolution. J. Geophys. Res.: Oceans 102 (C12), 26455–26470.

Grove, J.M., 2001. The initiation of the" Little Ice Age" in regions round the North Atlantic. Clim. Change 48, 53–82.

Gupta, A.K., Anderson, D.M., Overpeck, J.T., 2003. Abrupt changes in the Asian southwest monsoon during the Holocene and their links to the North Atlantic Ocean. Nature 421 (6921), 354–357.

Gupta, H.P., Sharma, C., 1986. Pollen Flora of North-West Himalaya. Indian Association of Palynostratigraphers, Lucknow (India), p. 181.

Harris, I.C., Jones, P.D., 2015. CRU TS3.23: Climatic Research Unit (CRU) Time-Series (TS) Version 3.23 of High Resolution Gridded Data of Month-by-month Variation in Climate (Jan. 1901–Dec. 2014). Centre for Environmental Data Analysis, University of East Anglia Climatic Research Unit; doi: 10.5285/4c7fdfa6-f176-4c58-acee-683d5e9d2ed5.
Hu, C., Henderson, G.M., Huang, J., Xie, S., Sun, Y., Johnson, K.R., 2008. Quantification of Holocene Asian monsoon rainfall from spatially separated cave records. Earth Planet. Sci. Lett. 266, 221–232.
Kaniewski, D., Marriner, N., Cheddadi, R., Guiot, J., Campo, E.V., 2018. The 4.2 ka BP event in the Levant. Clim. Past 14, 1529–1542.
Kar, R., Ranhotra, P.S., Bhattacharyya, A., Sekar, B., 2002. Vegetation vis-à-vis climate and glacial fluctuations of the Gangotri Glacier since the last 2000 years. Curr. Sci. 82, 347–351.
Kathayat, G., Cheng, H., Sinha, A., Berkelhammer, M., Zhang, H., Duan, P., Li, H., Li, X., Ning, Y., Edwards, R.L., 2018. Evaluating the timing and structure of the 4.2 ka event in the Indian summer monsoon domain from an annually resolved speleothem record from Northeast India. Clim. Past 14, 1869–1879.
Kathayat, G., Cheng, H., Sinha, A., Yi, L., Li, X., Zhang, H., Li, H., Ning, Y., Edwards, R.L., 2017. The Indian monsoon variability and civilization changes in the Indian subcontinent. Sci. Adv. 3, e1701296.
Keigwin, L.D., 1996. The little ice age and medieval warm period in the Sargasso Sea. Science 274, 1504–1508.
Klimenko, V.V., 2004. Sharp cooling of the Northern Hemisphere in the Early Subatlantic age (650–280 BC). Pages News 12, 13–15.
Kotlia, B.S., Ahmad, S.M., Zhao, J.X., Raza, W., Collerson, K.D., Joshi, L.M., Sanwal, J., 2012. Climatic fluctuations during the LIA and post-LIA in the Kumaun Lesser Himalaya, India: evidence from a 400 y old stalagmite record. Quat. Int. 263, 129–138.
Kotlia, B.S., Bhalla, M.S., Sharma, C., Rajagopalan, G., Ramesh, R., Chauhan, M.S., Mathur, P.D., Bhandari, S., Chacko, S.T., 1997. Palaeoclimatic conditions in the upper Pleistocene and Holocene Bhimtal-Naukuchiatal lake basin in south-central Kumaun, North India. Palaeogeogr. Palaeoclimatol. Palaeoecol. 130, 307–322.
Kotlia, B.S., Singh, A.K., Joshi, L.M., Dhaila, B.S., 2015. Precipitation variability in the Indian Central Himalaya during last ca. 4,000 years inferred from a speleothem record: Impact of Indian Summer Monsoon (ISM) and Westerlies. Quat. Int. 371, 244–253.
Kotlia, B.S., Singh, A.K., Zhao, J.X., Duan, W., Tan, M., Sharma, A.K., Raza, W., 2017. Stalagmite based high resolution precipitation variability for past four centuries in the Indian Central Himalaya: Chulerasim cave re-visited and data re-interpretation. Quat. Int. 444, 35–43.
Kripalani, R.H., Kulkarni, A., Sabade, S.S., 2003. Western Himalayan snow cover and Indian monsoon rainfall: A re-examination with INSAT and NCEP/NCAR data. Theor. Appl. Climatol. 74, 1–18.
Kumar, P., Chopra, S., Pattanaik, J.K., Ojha, S., Gargari, S., Joshi, R., Kanjilal, D., 2015. A new AMS facility at Inter University Accelerator Centre, New Delhi. Nucl. Instrum. Methods Phys. Res., Sect. B 361, 115–119.
Lamb, H.H., 1965. The early medieval warm epoch and its sequel. Palaeogeogr. Palaeoclimatol. Palaeoecol. 1, 13–37.
Laskar, A.H., Yadava, M.G., Ramesh, R., Polyak, V.J., Asmerom, Y., 2013. A 4 kyr stalagmite oxygen isotopic record of the past Indian Summer Monsoon in the Andaman Islands. Geochem. Geophys. Geosyst. 14, 3555–3566.
Leipe, C., Demske, D., Tarasov, P.E., Members, H.P., 2014. A Holocene pollen record from the northwestern Himalayan lake Tso Moriri: implications for palaeoclimatic and archaeological research. Quat. Int. 348, 93–112.
Liang, F., Brook, G.A., Kotlia, B.S., Railsback, L.B., Hardt, B., Cheng, H., Edwards, R.L., Kandasamy, S., 2015. Panigarh cave stalagmite evidence of climate change in the Indian Central Himalaya since AD 1256: Monsoon breaks and winter southern jet depressions. Quat. Sci. Rev. 124, 145–161.
Liu, F., Feng, Z., 2012. A dramatic climatic transition at ~4000 cal. yr BP and its cultural responses in Chinese cultural domains. The Holocene 22, 1181–1197.
Lone, A.M., Achyuthan, H., Shah, R.A., Sangode, S.J., Kumar, P., Chopra, S., Sharma, R., 2020. Paleoenvironmental shifts spanning the last~ 6000 years and recent anthropogenic controls inferred from a high-altitude temperate lake: Anchar Lake, NW Himalaya. The Holocene 30, 23–36.
MacDonald, G., 2011. Potential influence of the Pacific Ocean on the Indian summer monsoon and Harappan decline. Quat. Int. 229, 140–148.
Managave, S., Shimla, P., Yadav, R.R., Ramesh, R., Balakrishnan, S., 2020. Contrasting Centennial-Scale Climate Variability in High Mountain Asia Revealed by a Tree-Ring Oxygen Isotope Record From Lahaul-Spiti. Geophys. Res. Lett. 47.
Mann, M.E., 2002. Large-scale climate variability and connections with the Middle East in past centuries. Clim. Change 55, 287–314.
Mann, M.E., Zhang, Z., Rutherford, S., Bradley, R.S., Hughes, M.K., Shindell, D., Ammann, C., Faluvegi, G., Ni, F., 2009. Global signatures and dynamical origins of the Little Ice Age and Medieval Climate Anomaly. Science 326, 1256–1260.
Marshall, M.H., Lamb, H.F., Huws, D., Davies, S.J., Bates, R., Bloemendal, J., Boyle, J., Leng, M.J., Umer, M., Bryant, C., 2011. Late Pleistocene and Holocene drought events at Lake Tana, the source of the Blue Nile. Global Planet. Change 78, 147–161.
Martin-Puertas, C., Matthes, K., Brauer, A., Muscheler, R., Hansen, F., Petrick, C., Aldahan, A., Possnert, G., Van Geel, B., 2012. Regional atmospheric circulation shifts induced by a grand solar minimum. Nat. Geosci. 5, 397–401.
Mayewski, P.A., Rohling, E.E., Stager, J.C., Karlén, W., Maasch, K.A., Meeker, L.D., Meyerson, E.A., Gasse, F., van Kreveld, S., Holmgren, K., Lee-Thorp, J., 2004. Holocene climate variability. Quat. Res. 62, 243–255.
Moore, P.D., Webb, J.A., Collison, M.E., 1991. Pollen analysis. Blackwell Scientific Publications, Oxford.
Nesje, A., Dahl, S.O., 2003. The 'little ice age'–only temperature? The Holocene 13, 139–145.
Paasche, Ø., Løvlie, R., Dahl, S.O., Bakke, J., Nesje, A., 2004. Bacterial magnetite in lake sediments: late glacial to Holocene climate and sedimentary changes in northern Norway. Earth Planet. Sci. Lett. 223, 319–333.
Park, J., Park, J., Yi, S., Kim, J.C., Lee, E., Choi, J., 2019. Abrupt Holocene climate shifts in coastal East Asia, including the 8.2 ka, 4.2 ka, and 2.8 ka BP events, and societal responses on the Korean peninsula. Sci. Rep. 9, 1–16.
Phadtare, N.R., 2000. Sharp decrease in summer monsoon strength 4000–3500 cal yr BP in the Central Higher Himalaya of India based on pollen evidence from alpine peat. Quat. Res. 53, 122–129.
Polanski, S., Fallah, B., Befort, D.J., Prasad, S., Cubasch, U., 2014. Regional moisture change over India during the past Millennium: A comparison of multi-proxy reconstructions and climate model simulations. Global Planet. Change 122, 176–185.
Prasad, S., Anoop, A., Riedel, N., Sarkar, S., Menzel, P., Basavaiah, N., Krishnan, R., Fuller, D., Plessen, B., Gaye, B., Röhl, U., 2014. Prolonged monsoon droughts and links to Indo-Pacific warm pool: A Holocene record from Lonar Lake, central India. Earth Planet. Sci. Lett. 391, 171–182.
Ran, M., Chen, L., 2019. The 4.2 ka BP climatic event and its cultural responses. Quat. Int. 521, 158–167.
Ranhotra, P.S., Bhattacharyya, A., Kar, R., Sekar, B., 2001. Vegetational and Climatic Changes around Gangotri Glacier during Holocene. In: National Symposium Role of Earth Sciences in Integrated Development and Related Societal Issues, Lucknow, vol. 3, p. 67. Geological Survey of India.
Ranhotra, P.S., Sharma, J., Bhattacharyya, A., Basavaiah, N., Dutta, K., 2018. Late Pleistocene-Holocene vegetation and climate from the palaeolake sediments, Rukti valley, Kinnaur, Himachal Himalaya. Quat. Int. 479, 79–89.
Rawat, S., Gupta, A.K., Sangode, S.J., Srivastava, P., Nainwal, H.C., 2015. Late Pleistocene-Holocene vegetation and Indian summer monsoon record from the Lahaul, northwest Himalaya, India. Quat. Sci. Rev. 114, 167–181.
Rowan, A.V., 2017. The 'Little Ice Age' in the Himalaya: A review of glacier advance driven by Northern Hemisphere temperature change. The Holocene 27, 292–308.
Sandeep, K., Shankar, R., Warrier, A.K., Yadava, M.G., Ramesh, R., Jani, R.A., Weijian, Z., Xuefeng, L., 2017. A multi-proxy lake sediment record of Indian summer monsoon variability during the Holocene in southern India. Palaeogeogr. Palaeoclimatol. Palaeoecol. 476, 1–14.
Sanwal, J., Kotlia, B.S., Rajendran, C., Ahmad, S.M., Rajendran, K., Sandiford, M., 2013. Climatic variability in Central Indian Himalaya during the last 1800 years: Evidence from a high resolution speleothem record. Quat. Int. 304, 183–192.
Sharma, M.C., Owen, L.A., 1996. Quaternary glacial history of NW Garhwal, central Himalayas. Quat. Sci. Rev. 15, 335–366.
Sharma, R., Umapathy, G.R., Kumar, P., Ojha, S., Gargari, S., Joshi, R., Chopra, S., Kanjilal, D., 2019. Ams and upcoming geochronology facility at inter university accelerator centre (IUAC), New Delhi, India. Nucl. Instrum. Methods Phys. Res., Sect. B 438, 124–130.
Shekhar, M., Bhardwaj, A., Singh, S., Ranhotra, P.S., Bhattacharyya, A., Pal, A.K., Roy, I., Martín-Torres, F.J., Zorzano, M.P., 2017. Himalayan glaciers experienced significant mass loss during later phases of little ice age. Sci. Rep. 7, 1–14.
Shukla, T., Mehta, M., Jaiswal, M.K., Srivastava, P., Dobhal, D.P., Nainwal, H.C., Singh, A.K., 2018. Late Quaternary glaciation history of monsoon-dominated Dingad basin, central Himalaya, India. Quat. Sci. Rev. 181, 43–64.
Singh, D.S., Tangri, A.K., Kumar, D., Dubey, C.A., Bali, R., 2017. Pattern of retreat and related morphological zones of Gangotri Glacier, Garhwal Himalaya, India. Quat. Int. 444, 172–181.
Singh, S., Gupta, A.K., Rawat, S., Bhaumik, A.K., Kumar, P., Rai, S.K., 2021. Paleomonsoonal shifts during 13700 to 3100 yr BP in the central Ganga Basin, India with a severe arid phase at 4.2 ka. Quat. Int.
Sinha, A., Berkelhammer, M., Stott, L., Mudelsee, M., Cheng, H., Biswas, J., 2011a. The leading mode of Indian Summer Monsoon precipitation variability during the last millennium. Geophys. Res. Lett. 38.
Sinha, A., Stott, L., Berkelhammer, M., Cheng, H., Edwards, R.L., Buckley, B., Aldenderfer, M., Mudelsee, M., 2011b. A global context for megadroughts in monsoon Asia during the past millennium. Quat. Sci. Rev. 30, 47–62.
Srivastava, P., Agnihotri, R., Sharma, D., Meena, N., Sundriyal, Y.P., Saxena, A., Bhushan, R., Sawlani, R., Banerji, U.S., Sharma, C., Bisht, P., 2017. 8000-year monsoonal record from Himalaya revealing reinforcement of tropical and global climate systems since mid-Holocene. Sci. Rep. 7, 1–10.
Staubwasser, M., Sirocko, F., Grootes, P.M., Erlenkeuser, H., 2002. South Asian monsoon climate change and radiocarbon in the Arabian Sea during early and middle Holocene. Paleoceanography 17, 15–21.
Steinhilber, F., Abreu, J.A., Beer, J., Brunner, I., Christl, M., Fischer, H., Heikkilä, U., Kubik, P.W., Mann, M., McCracken, K.G., Miller, H., 2012. 9,400 years of cosmic radiation and solar activity from ice cores and tree rings. Proc. Natl. Acad. Sci. 109, 5967–5971.
Steinhilber, F., Beer, J., Fröhlich, C., 2009. Total solar irradiance during the Holocene. Geophys. Res. Lett. 36.
Stuiver, M., Grootes, P.M., Braziunas, T.F., 1995. The GISP2 δ18O climate record of the past 16,500 years and the role of the sun, ocean, and volcanoes. Quat. Res. 44, 341–354.
Thompson, L.O., Yao, T., Davis, M.E., Henderson, K.A., Mosley-Thompson, E., Lin, P.N., Beer, J., Synal, H.A., Cole-Dai, J., Bolzan, J.F., 1997. Tropical climate instability: The last glacial cycle from a Qinghai-Tibetan ice core. Science 276, 1821–1825.
Tiwari, M., Ramesh, R., Somayajulu, B.L.K., Jull, A.J.T., Burr, G.S., 2006. Paleomonsoon precipitation deduced from a sediment core from the equatorial Indian Ocean. Geo-Mar. Lett. 26, 23–30.

Trivedi, A., Kotlia, B.S., Joshi, L.M., 2011. Mid-Holocene vegetation shifts and climate change in the temperate belt of Garhwal Himalaya. Palaeobotanist 60, 291–298.

Vishnu-Mittre, Sharma, C., 1984. Vegetation and climate during the last glaciation in the Kathmandu Valley, Nepal. Pollen et Spores 26, 69–94.

Walker, M., Gibbard, P., Head, M.J., Berkelhammer, M., Björck, S., Cheng, H., Cwynar, L. C., Fisher, D., Gkinis, V., Long, A., Lowe, J., 2019. Formal subdivision of the Holocene series/epoch: a summary. J. Geol. Soc. India 93, 135–141.

Walker, M., Head, M.J., Berkelhammer, M., Björck, S., Cheng, H., Cwynar, L., Fisher, D., Gkinis, V., Long, A., Lowe, J., Newnham, R., 2018. Formal ratification of the subdivision of the Holocene Series/Epoch (Quaternary System/Period): two new Global Boundary Stratotype Sections and Points (GSSPs) and three new stages/ subseries. Episodes 41, 213–223.

Walker Mike, J.C., Berkelhammer, M., Björck, S., Les, C., Cwynar David, A., Fisher, A., Long, J., Jone, J., Lowe, R.M., Newnham, S.O., Rasmussen, H.W., 2012. Formal subdivision of the Holocene Series/Epoch: a Discussion Paper by a Working Group of INTIMATE (Integration of ice-core, marine and terrestrial records) and the Subcommission on Quaternary Stratigraphy (International Commission on Stratigraphy). J. Quat. Sci. 27, 649–659.

Wan, G., Zhang, D.D., Zhang, F., Huang, R., 2004. Environmental records of lacustrine sediments in different time scales: Sediment grain size as an example. Sci. China, Ser. D Earth Sci. 47, 954–960.

Wanner, H., Mercolli, L., Grosjean, M., Ritz, S.P., 2015. Holocene climate variability and change; a data-based review. J. Geol. Soc. 172, 254–263.

Wünnemann, B., Demske, D., Tarasov, P., Kotlia, B.S., Reinhardt, C., Bloemendal, J., Diekmann, B., Hartmann, K., Krois, J., Riedel, F., Arya, N., 2010. Hydrological evolution during the last 15 kyr in the Tso Kar lake basin (Ladakh, India), derived from geomorphological, sedimentological and palynological records. Quat. Sci. Rev. 29, 1138–1155.